

CONF-980402--

EXPERIMENTAL INVESTIGATIONS OF THE SNEDDON SOLUTION AND AN
IMPROVED SOLUTION FOR THE ANALYSIS OF NANOINDENTATION DATA

JACK C. HAY, G.M. PHARR

Accepted for publication in Materials Research Society Symposium Proceedings, 1998

RECEIVED

AUG 13 1998

OSTI

MASTER *just*

DISTRIBUTION OF THIS DOCUMENT IS UNLIMITED

DISCLAIMER

This report was prepared as an account of work sponsored by an agency of the United States Government. Neither the United States Government nor any agency thereof, nor any of their employees, makes any warranty, express or implied, or assumes any legal liability or responsibility for the accuracy, completeness, or usefulness of any information, apparatus, product, or process disclosed, or represents that its use would not infringe privately owned rights. Reference herein to any specific commercial product, process, or service by trade name, trademark, manufacturer, or otherwise does not necessarily constitute or imply its endorsement, recommendation, or favoring by the United States Government or any agency thereof. The views and opinions of authors expressed herein do not necessarily state or reflect those of the United States Government or any agency thereof.

DISCLAIMER

Portions of this document may be illegible in electronic image products. Images are produced from the best available original document.

EXPERIMENTAL INVESTIGATIONS OF THE SNEDDON SOLUTION AND AN IMPROVED SOLUTION FOR THE ANALYSIS OF NANOINDENTATION DATA

JACK C. HAY*, G.M. PHARR**

* I.B.M. Research, T.J. Watson Research Center, P.O. Box 218, Yorktown Heights, NY, 10598-0218

** Department of Materials Science, Rice University, 6100 Main Street; M.S. 321, Houston, TX 77005-1892

ABSTRACT

The Sneddon solution, as it is implemented in the Oliver-Pharr method, deviates from the indentation experimental data in a manner which depends on both the indenter angle and the Poisson ratio of the sample. These effects are demonstrated experimentally by performing indentations in tungsten and aluminum using a cube-cube corner indenter where the effects are exacerbated by the small indenter angle. The first objective was to experimentally support and validate an approximate analytical solution in conjunction with finite element simulations which illustrate the Poisson ratio and indenter angle effects. Second, a review of data analysis procedures is presented which leads to a better understanding of the systematic errors which percolate through in the measurement of Young's modulus and hardness.

INTRODUCTION

A recent study [1-3] of the Sneddon solution for elastic contact by a rigid cone [4-5] indicates that the shape of the deformed surface is different from the desired indenter profile within the contact radius; specifically, the final deformed surface is cusp-shaped [1-3] rather than linear in the contact region. The boundary conditions of the Sneddon problem are such that z-displacements are imposed within the contact radius, but the radial positions are not constrained to the shape of the indenter. The amount by which the deformed surface deviates from the modeled indenter shape depends on the included indenter angle and the Poisson ratio of the material.

Finite element simulations [1-3] for the elastic contact problem corroborate these interpretations of the Sneddon solution. When the exact Sneddon boundary conditions are employed in a finite element simulation, the final nodal positions are consistent with the deformed surface profile given by Sneddon. An important consequence is that the Sneddon solution underestimates the actual loads and contact radii for a rigid conical indenter. One can expect deviations of up to 14% and 49% in the contact area of conical indenters with the same depth-to-area ratios as the Berkovich and cube-corner indenters, respectively.

As detailed elsewhere [1], the Sneddon solution used for the analysis of indentation load-displacement data does not adequately describe contact by a rigid cone and should be rewritten as

$$S = \frac{2}{\sqrt{\pi}} \beta \frac{E}{(1-\nu^2)} \gamma \sqrt{A} \quad (1)$$

where S is the contact stiffness, E is the Young's modulus, ν is the Poisson ratio, β is a geometrical correction accounting for the cross-sectional shape of the indenter, and A is the projected contact area. This is different from the original Sneddon solution because it contains γ , a correction factor which accounts for the fact that Sneddon's boundary conditions result in a cusp-shaped deformation within the contact radius rather than the prescribed conical shape. The correction factor depends on the Poisson ratio of the material and the indenter half angle as given by [1]

$$\gamma = 1 + \frac{(1-2\nu)}{4(1-\nu)\tan\phi} \quad (2)$$

Therefore, the actual area of the cusp-shaped surface and the area of the ideally rigid indenter differ by a factor of γ^2 . In the limit of a blunt indenter ($\phi=90^\circ$) or for materials where $\nu=0.5$, the correction factor is equal to 1.

Pharr, Oliver and Brotzen [7] demonstrated that the contact stiffness determined from $S=dP/dh$ depends only on the contact area and the Young's modulus of the material. While the

load determined by Sneddon's analysis will depend on the indenter geometry, the contact stiffness does not. The correction factor, γ , presented by Hay et al. [1] is defined such that the deformed surface is still cusp-shaped, but passes through the correct contact radius. In this case, the contact stiffness should be correct according to Pharr et al. [7].

The objectives of the current paper are twofold. First, we wish to test and validate the approximate analytical solution given by Eqs. (1) and (2) by calibrating a cube-corner diamond tip. Secondly, an analysis of the errors incurred by using the Sneddon solution uncorrected for the Poisson ratio and indenter angle influences is presented. Using the methods developed by Oliver and Pharr [6], systematic errors in the contact area percolate through the calculations of E and H , but are minimized when testing with blunt indenters.

EXPERIMENTAL

Nanoindentation experiments were conducted using a Nanoindenter IITM, a load and depth sensing instrument capable of precise positioning of indentations. The instrument's utility lies in the fact that indentations only a few nanometers deep can yield accurate measurements of the loads and displacements used to evaluate Young's modulus and hardness. The theoretical resolutions of the machine are 0.04 nm and 75 nN for the displacement and load measurements.

All indentation experiments were conducted with the cube-corner indenter as follows. The indenter tip approached the samples at a rate of 10 nm/s and surface contact was detected by a change in contact stiffness. The indenter was then driven into the sample at 1 nm/s to a depth of 10 nm, 2 nm/s to a depth of 30 nm, 4 nm/s to a depth of 70 nm, and 8 nm/s to a maximum load of 153 mN. The indenter was then withdrawn at a rate of 8 nm/s to 10% of the maximum load, and the load was held constant for 100 seconds providing a segment to determine the thermal drift of the system. The indenter was then completely unloaded.

The continuous stiffness measurement (CSM) option was used to obtain continuous contact stiffness measurements as the indenter was driven into the sample. This technique measures the contact stiffness at many points along the loading curve, differing from the conventional load-displacement-time method where only one contact stiffness measurement is made from the unloading portion of the experiment at P_{max} . Thus, one indentation experiment can be used to provide all of the information which would be measured from several conventional load-displacement-time experiments performed at various peak loads. For the experiments in this study, the CSM imposed a 1 nm oscillation at 45 Hz on the loading curve. The dynamic response modeled as a mass-spring-dashpot system yielded the contact stiffness used in Eq. (1).

The equations which will be of importance to the analysis of experimental data are Eqs. (1) and (2) above and

$$H = \frac{P}{A}, \quad (3)$$

where H is the hardness, P is the load and A is the contact area.

Experiments were conducted on two materials: aluminum and tungsten. A single crystal of aluminum was used as a calibrating medium for the cube-corner tip area function. This tip geometry was selected because it has a small equivalent cone angle which exacerbates the indenter angle effect in Eq. (2). An area function was established by the Oliver-Pharr method [6], assuming $\gamma=1$ in Eq. (1), and was then implemented to evaluate the hardness of tungsten. The area function was then reevaluated including the correction factor, γ , in Eq. (2), providing a better estimate of the true tip shape. Scanning electron micrographs provided direct evidence of the final contact area to compare with the area function.

RESULTS

In the determination of an area function, which describes the cross-sectional area of the indenter tip as a function of distance from the apex, two quantities are measured independently. First, the contact area is determined from Eq. (1). Through careful selection of a calibrating material for which the Young's modulus and Poisson's ratio are known, experimental contact stiffnesses and Eq. (1) yield an estimate of the total contact area under load. However, if γ is assumed to be 1.0, the area deduced by this procedure is larger than the actual area, A_{actual} , by γ^2 . The second quantity required for experimental calibration of the indenter tip is the contact depth,

which follows from an independent procedure developed by Oliver and Pharr [6], adapted from earlier work by Doerner and Nix [9]. We begin by discussing the errors introduced in the contact area and then proceed to the errors in the contact depth. The single crystal of aluminum used as a calibration sample does not tend to pile-up, has minimal elastic anisotropy, and does not crack during indentation experiments with the cube-corner indenter.

For clarity, the Sneddon solution used by Oliver and Pharr [6] for determining the contact area is rewritten, without the γ factor, as

$$A = \left[S \frac{\sqrt{\pi}}{2} \frac{1}{\beta} \frac{(1-\nu^2)}{E} \right]^2, \quad (4)$$

where the terms on the right hand side are either known material properties or are measurable. In this case a Young's modulus of 70.3 GPa for aluminum was used and the Poisson ratio was 0.345 [8]. This step yields a contact area at each data point during the loading portion of the experiment.

The second quantity required for the determination of an area function is the contact depth, or the distance from the indenter tip to the point where the deformed material and indenter lose contact. The Oliver-Pharr method [6] prescribes one method for determining the contact depth from the contact stiffness, the load, and total depth, all of which are all measurable from the raw data. At each point along the loading curve the contact depth, h_c , is determined from

$$h_c = h_{\text{total}} - \varepsilon \frac{P}{S} \quad (5)$$

where ε is a geometric constant [6] equal to 1.0 for a flat punch, 0.72 for a conical indenter, and 0.75 for a paraboloid of revolution. Oliver and Pharr reported that their data for the Berkovich tip was best described when $\varepsilon = 0.75$. The same value has been adopted here for use with the cube-corner indenter.

The area function is determined by plotting the calculated contact area, A , against the contact depth, h_c . While Oliver and Pharr suggest fitting the data to a ninth order polynomial, such a function becomes overspecialized beyond about the first 5 terms. One indication of an overspecialized curve fit is large constants, C_i , of alternating signs for the last terms. Therefore, we have truncated the last terms and perform only a fifth order polynomial curve fit using

$$A(h_c) = C_1 h_c^2 + C_2 h_c + C_3 h_c^{1/2} + C_4 h_c^{1/4} + C_5 h_c^{1/8} \quad (6)$$

where C_1 through C_5 are least squares fitting constants.

The area function for the cube-corner indenter determined with no correction factor is presented in Figure 1 as curve 'A'. For comparison, the area function for a perfect cube-corner tip is presented in Figure 1 as a dashed curve. There are three explanations for the apparent discrepancy between the calculated area function and the ideal tip: (1) the calculated area, A , is overestimated, (2) the calculated contact depths are underestimated, or (3) the tip was not ground to the characteristic shape of a cube-corner.

To address the first point, an independent measurement of the contact area in aluminum was made using SEM images. Figure 2 is a micrograph of a 153 mN indentation in single crystal aluminum produced with a cube-corner indenter. A trace of the indentation perimeter reveals a contact area of 537 μm^2 . This area is presented in Figure 1 as a solid horizontal line. It is seen that the area determined by Eq. (4) clearly overestimates the actual contact area at maximum load, because of an effect due to the Poisson ratio and indenter angle, accounted for in γ , which has not yet been included in the calculation of A .

By inspection of Eqs. (4) and (1), the quantity which is actually determined from the right-hand-side of Eq. (4) is $\gamma^2 A$ not A . In the development of the technique by Oliver and Pharr, γ was implicitly assumed to be equal to 1. According to Eq. (2), though, $\gamma = 1.13$ for a material with a Poisson ratio equal to 0.345 and an equivalent cone angle of 42.28°. Therefore, all of the areas used in the area function in Figure 1 are overestimated by a factor γ^2 , or a factor of 1.28. A revised area function is included in Figure 1 where the areas have been reduced by a factor of 1.28 and is denoted as curve 'B'.

Note that the area for curve 'B' at the largest depth compares favorably with the area measured by SEM. However, a second factor which may introduce error into the area function is in the determination of the contact depth. It has been assumed that the elastic contact theory used by Oliver and Pharr to develop Eq. (5) will yield the correct contact depth even for a material

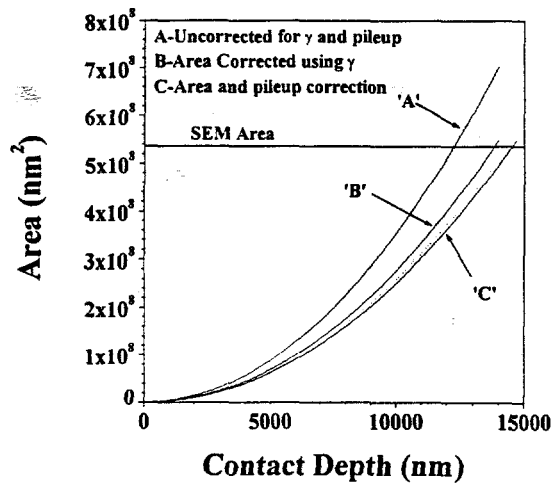


Figure 1. Cube-corner indenter area function evaluated using tungsten metal. Area function accounts for gamma and pileup.

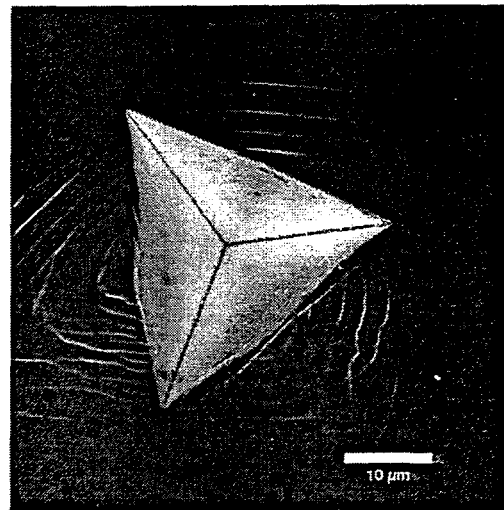


Figure 2. SEM image of a 153 mN indentation impression in an aluminum single crystal using the cube corner diamond tip.

which has a large plastic component. When the material piles up around the indenter, though, the deformed surface will increase the actual contact depth.

In the case of a three sided pyramidal indenter, such as the Berkovich and cube-corner tips, the pile-up is not uniform about the indentation. Referring to Figure 2, pile-up along the sides of the impression is manifested in a "bulging" which deviates from the assumed linear sides. Since the micrograph itself provides the plan-view area of the contact impression, one can see that the pile-up results in a larger contact area than is predicted from elastic contact theory. Another way of interpreting the significance of the pile-up is that the effective contact depth is larger than that predicted by Eq. (5). It is interesting to note from Figure 1 that the contact depths predicted from Eq. (5) are in fact less than that expected for the ideal cube-corner tip.

It is proposed here that one may determine an approximate relationship between the elastic contact depth from Eq. (5) and the effective, or average, contact depth resulting from the pile-up evidenced in the SEM micrograph. However, there are several assumptions which must first be addressed. First, it is assumed that the area measured by SEM is representative of the contact area under load; that is, the elastic recovery during the unloading portion of the experiment results in vertical displacements, only. Secondly, it must be assumed that there is minimal pile-up at the corners of the impression. Atomic force microscopy has demonstrated that at least for the aluminum single crystal used here, this is a valid assumption. This assumption is required in order to assume that the corner-to-corner area in Figure 2 corresponds with the contact depth determined from Eq. (5). Given these two assumptions, the effective contact depth can be determined from geometric similarity by

$$h_{c,\text{effective}} = h_c \frac{A_{\text{actual}}}{A_{c-c}}, \quad (7)$$

where A_{actual} is the contact area determined from a trace of the indentation perimeter in Figure 2, and A_{c-c} is the corner-to-corner area in Figure 2.

If one accepts that the pile-up character is self-similar due to the self-similarity of the indenter, then a constant scaling factor exists between the elastic contact depth and the effective contact depth. For this particular case of indentation in aluminum by a cube-corner indenter, that scaling factor is approximately 1.05. Therefore, all of the contact depths determined by Eq. (5) are too small by 5%. When the contact depths in Figure 1 are increased by a factor of 1.05, a final area function is established which accounts for the Poisson ratio, indenter half angle, and pileup effects. Note in Figure 1 that this revised area function presented as curve 'C' agrees very well with the ideal area function for a cube-corner indenter.

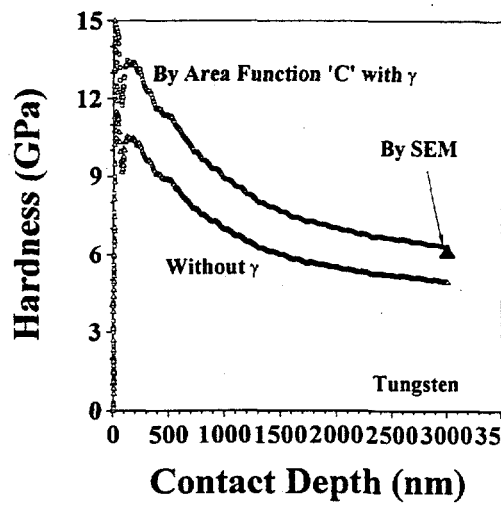


Figure 3. Hardness of tungsten metal as measured using the with the corrected and uncorrected area functions. The large triangle point was measured by SEM.

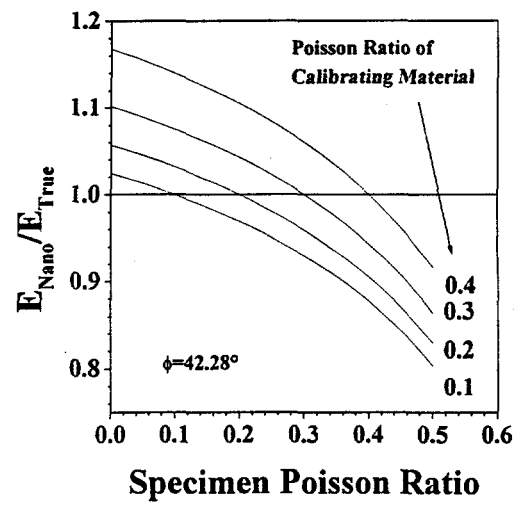


Figure 4. Error in the Young's modulus due to differences in the Poisson ratio between the calibrating material and specimen of interest for the cube corner tip.

DISCUSSION

Having established that the accepted methods of experimentally calibrating area functions actually overestimate the true contact area, the next task is to determine the severity of errors incurred by using an incorrect area function to determine the Young's modulus, E , and the hardness, H . To address this question, a tungsten sample was indented with the cube-corner diamond tip, and the Young's modulus and hardness were evaluated using the uncorrected and corrected area functions in Figure 1.

Errors in the area function enter explicitly when the hardness is evaluated. When the area function is calibrated according to Oliver-Pharr [6], the areas are too large by a factor of γ^2 . The errors which can be expected in the measured hardness are easily determined from,

$$\%Error = 100\left(1 - \frac{1}{\gamma^2}\right). \quad (8)$$

When the tip is calibrated using aluminum with a Poisson ratio of 0.345, the expected error in the measured hardness of other materials is approximately 22%

The hardness of the tungsten sample, determined from Eq. (3), is plotted in Figure 3. The large triangle represents the actual hardness where the area was measured directly by SEM. Note that the final hardness measured by the nanoindentation analysis using an uncorrected area function underestimates the actual hardness as determined from SEM methods. Referring back to Figure 1, this is expected since the uncorrected area function overestimates the actual contact area. When the corrected area function in Figure 1 is used to determine the hardness, the hardness at maximum depth is similar to the actual hardness measured by SEM analysis, as shown by the square data points in Figure 3. It is interesting to note the close agreement between the analytical and actual hardness measurements at the maximum penetration depth.

The influence of the γ^2 term in the area function is not so straight forward when considering the effects on the Young's modulus. Recall that the area function determined by the Oliver-Pharr method actually gives $\gamma^2 A$. Therefore, when the contact area is determined from an uncorrected area function and is used with Eq. (1) for a sample of an unknown Young's modulus, a γ factor has actually been included. While γ is not inserted explicitly, the uncorrected contact area taken from the area function is the true contact area multiplied by γ^2 of the sample used to calibrate the tip. The data is actually analyzed according to

$$S_m = \frac{2}{\sqrt{\pi}} \beta \frac{E_m}{(1 - \nu_m^2)} \sqrt{\gamma_{cs}^2 A}, \quad (9)$$

where the included γ term is for the calibration sample (cs) and not for the sample of interest (m). Ironically, when the Poisson ratios of the calibration sample and the sample of interest are the

same, one can still obtain the correct Young's modulus by the current methods even though the area function is not correct, by virtue of the materials having the same γ factor.

To examine the magnitude of the errors that result from calibrating with a material of one Poisson ratio and testing a material with a different Poisson ratio, it is constructive to consider the ratio of Eq. (1) for the calibration sample (cs) to Eq. (1) for a sample of interest (m). The influence of a mismatch in ν is given by

$$E_m = E_{cs} \frac{S_m \gamma_{cs}}{S_{cs} \gamma_m}. \quad (10)$$

The error resulting from using the uncorrected area functions is then γ_{cs}/γ_m . For clarity, this error due to the mismatch in Poisson ratios has been plotted in Figure 4 for the cube-corner geometry ($\phi=42.28^\circ$).

The implications for Young's modulus measurement are minimal for practical indentation with tips of large half-included angles, such as 70.32° for the Berkovich tip, even for relatively large disparity in the Poisson ratios. Referring to Eqs. (2) and (10), the error which results from calibrating the area function using a material with a Poisson ratio of 0.3 and then testing a material with a Poisson ratio of 0.2 is approximately 1.5%. However, the error may explain difficulties in calibrating the sharper cube-corner indenter tips, since the error is closer to 8% for the same disparity in Poisson ratios.

CONCLUSIONS

A companion paper examines the theoretical foundations of the Sneddon solution and firmly establishes that the experimental indentation community has misinterpreted the Sneddon solution. The Sneddon solution as used by Oliver and Pharr overestimates the actual contact area, especially for small Poisson ratios or for sharp indenters. This experimental study demonstrates by example that this misinterpretation results in incorrect assessments of area functions, and ultimately results in the incorrect measurement of the Young's moduli and hardnesses which rely on the area function. However, a simple, approximate analytical correction factor has been developed which can be incorporated into the Sneddon solution to correctly determine the contact area. By incorporating the correction factor into the analysis, an improved solution for the analysis of experimental data is established.

ACKNOWLEDGMENTS

This research was sponsored in part by the Division of Materials Sciences, U.S. Department of Energy, under contract DE-AC05-96OR22464 with Lockheed Martin Energy Research Corp., through the SHaRE Program under contract DE-AC05-76OR00033 with Oak Ridge Associated Universities, and by an appointment (JCH) to the ORNL Postdoctoral Research Associates Program administered jointly by the Oak Ridge Institute for Science and Education and ORNL.

REFERENCES

1. J.C. Hay, A. Bolshakov, G.M. Pharr, submitted to Mat. Res. Soc. Symp. Proc. 'T', Spring 1998.
2. A. Bolshakov, G.M. Pharr, Mat. Res. Soc. Symp. Proc., 436, 189-194 (1997).
3. A. Bolshakov, W.C. Oliver, G.M. Pharr, J. Mater. Res., 11, 760-768 (1996).
4. I.N. Sneddon, Int. J. Engng. Sci., 3, 47-57 (1965).
5. I.N. Sneddon, Fourier Transforms. McGraw-Hill Book Company, Inc., 1951, pp. 450-467.
6. W.C. Oliver, G.M. Pharr, J. Mater. Res., 7, 1564-1583 (1992).
7. G.M. Pharr, W.C. Oliver, F.R. Brotzen, J. Mater. Res., 7, 613-617 (1992).
8. R.W. Hertzberg, Deformation and Fracture Mechanics of Engineering Materials, (John Wiley & Sons, New York, 1989) p. 7.
9. M.F. Doerner, W.D. Nix, J. Mater. Res., 1, 601 (1986).